

Passivity preserving moment-based finite-order hydrodynamic model identification for wave energy applications

Original

Passivity preserving moment-based finite-order hydrodynamic model identification for wave energy applications / Faedo, N.; Pena-Sanchez, Y.; Ringwood, J. V.. - (2019), pp. 351-359. (3rd International Conference on Renewable Energies Offshore (RENEW 2018)).

Availability:

This version is available at: 11583/2988072 since: 2024-04-24T11:58:52Z

Publisher:

3rd International Conference on Renewable Energies Offshore (RENEW 2018)

Published

DOI:

Terms of use:

This article is made available under terms and conditions as specified in the corresponding bibliographic description in the repository

Publisher copyright

(Article begins on next page)

Passivity preserving moment-based finite-order hydrodynamic model identification for wave energy applications

Nicolás Faedo, Yeraí Peña-Sánchez & John V. Ringwood

Centre for Ocean Energy Research, Maynooth University, Maynooth, Co., Kildare, Ireland

ABSTRACT: The dynamics of a Wave Energy Converter (WEC) are described in terms of an integro-differential equation, particularly, of the convolution class. This convolution term, which is associated with fluid memory effects of the radiation forces acting on the WEC, represents a major drawback both for simulation, analysis and control design for WECs. Recently, a moment-matching based method to approximate this convolution term by a parametric model was presented in (Faedo et al. 2018). Such a technique allows the computation of a model that can match exactly the frequency response of the original system at a set of chosen frequencies. Though the models computed by this strategy are almost always inherently passive, the proposed method does not specifically ensure *passivity*, which is one of the main physical properties of the radiation subsystem. This paper describes an extension of the moment-based methodology presented in (Faedo et al. 2018) which guarantees a passive finite-order representation for the radiation kernel based on moment-matching. Moreover, we illustrate the applicability of the method by the means of a numerical example with a particular WEC.

1 INTRODUCTION

The dynamics of Wave Energy Converters (WECs) can be modelled (and described) using a specific set of hydrodynamic parameters which relate to the well-known Cummins' equation (Cummins 1962). These parameters are virtually always computed using Boundary Element Methods (BEMs) (Penalba et al. 2017). Examples of the most popular BEM hydrodynamic codes are the open-source software NEMOH (Babarit and Delhommeau 2015) and the commercially available code WAMIT (Lee 1995). The major drawback behind BEMs is that the results are computed in the frequency-domain and, hence, can only characterise the steady-state motion of the WEC under study. Although, for some applications, this steady-state formulation may be sufficient, a more comprehensive approach considers a time-domain formulation of the WEC dynamics, following Cummins' equation. This time-domain equation has a direct relation with the hydrodynamic coefficients computed by BEMs. The resulting dynamical model is an integro-differential equation, which contains a convolution term accounting for the fluid memory effects associated with radiation forces acting on the body of the device.

Unfortunately, such a convolution term represents a difficulty when it comes to motion simulation, estimation, and/or control system design. In the motion simulation case, the convolution

operator basically entails a considerable computational effort in comparison with finite-order parametric models. From both estimation and control theory perspectives, such a term is inconvenient, since modern estimation and control strategies are based on the availability of a representation of the system in (at least) local coordinates of a suitable state-space manifold. In fact, the majority of the control strategies considered for wave energy applications require of a parametric approximation of the radiation convolution term (Faedo et al. 2017), with some notable exceptions, such as (Bacelli and Ringwood 2015) and (Faedo et al. 2018).

The finite-order model that approximates the convolution term must respect the physical properties behind radiation forces. Among the physical properties of this subsystem (see Table 1), one can find that radiation forces are *passive*.

Table 1. Properties of the radiation force kernel k .

Property	Significance on k
$\lim_{\omega \rightarrow 0} K(j\omega) = 0$	It has zeros at the origin.
$\lim_{\omega \rightarrow +\infty} K(j\omega) = 0$	Strictly proper
$\lim_{t \rightarrow 0^+} k(t) \neq 0$	Relative degree 1
$\lim_{t \rightarrow +\infty} k(t) = 0$	BIBO stable
$K(j\omega)$ is positive real	Passive ¹

Informally, a system is said to be passive if it cannot produce energy. This property derives from the fact that radiation forces are inherently dissipative (Damaren 2000). Besides being an intrinsic physical property of the radiation force subsystem (and thus should be respected by the finite-order approximation), passivity has an impact on the stability of the WEC mathematical model. This is the main motivation behind this study, and is further discussed in Section 4.2.

Several methods have been proposed to obtain a finite-order approximation for the radiation convolution term, with reviews available in studies such as (Taghipour et al. 2008) and (Roessling and Ringwood 2015). In particular, a moment-matching based strategy has recently been presented in (Faedo et al. 2018), which has a set of attractive properties: this method allows the computation of a model that *exactly* matches the frequency response of the target radiation kernel at a set of specific (chosen) frequencies, providing a robust and efficient method to compute a state-space representation for the dynamics of a WEC. Moreover, this methodology can be applied for both the radiation force subsystem or the complete force-to-motion dynamics. Despite the fact that matching the behaviour of the target system at important frequencies (such as, for example, the resonant frequency of the device), potentially helps to retain key properties of the system under analysis, the method presented in (Faedo et al. 2018) does not explicitly guarantee passivity (although, in most cases, the obtained model with this strategy is inherently passive). This study proposes a modification of the methodology developed in (Faedo et al. 2018), based on the moment-matching results presented in (Ionescu and Astolfi 2010), which *ensures* the passivity condition when computing an approximated model for the radiation force subsystem, while keeping, at the same time, the benefit of selecting key frequencies in the identification process.

The remainder of this paper is organised as follows. Section 2 presents the theoretical basis behind moment-matching, while Section 3 deals with WEC modelling. The passivity-preserving moment-based identification method is developed in Section 4. Finally, a numerical example is presented in Section 5, with the relevant conclusions of the strategy summarised in Section 6.

Notation

Standard notation is used through this paper, with some exceptions further detailed in this preliminary section. \mathbb{R}^+ (\mathbb{R}^-) denotes the set of non-negative (non-positive) real numbers. \mathbb{C}^0 denotes the set of pure-imaginary complex numbers and \mathbb{C}^- denotes the set of complex numbers

with negative real part. The symbol 0 stands for any zero element, according to the context. The symbol \mathbb{I}_n denotes an order n identity matrix. The spectrum of a matrix $A \in \mathbb{R}^{n \times n}$, i.e. the set of its eigenvalues, is denoted as $\sigma(A)$. The symbol \oplus denotes the direct sum of n matrices, i.e. $\oplus_{i=1}^n A_i = \text{diag}(A_1, A_2, \dots, A_n)$. The notation $\Re\{z\}$ and $\Im\{z\}$, with $z \in \mathbb{C}$, stands for the *real-part* and the *imaginary-part* operators, respectively. The expression $\|x\|_b$, with $x \in \mathbb{C}^{n \times 1}$, denotes the ℓ^2 -norm of the complex-valued vector x . The H_∞ -norm of a transfer function $G(s): \mathbb{C} \rightarrow \mathbb{C}$ is denoted as $\|G(s)\|_\infty$. The convolution between two functions $f(t)$ and $g(t)$ over a finite range $[0, t]$, i.e. $\int_0^t f(\tau)g(t-\tau)d\tau$ is denoted as $f * g$. The Fourier transform of a function $f(t) \in L^2(\mathbb{R})$ is denoted by $\mathcal{F}\{f(t)\} \equiv F(j\omega)$, while the Laplace transform is denoted as $\mathcal{L}\{f(t)\} \equiv F(s)$, where $L^2(\mathbb{R})$ is the function space of all real-valued square-integrable functions. Finally, the symbol $\varepsilon_n \in \mathbb{R}^{n \times 1}$ denotes a vector with odd components equal to 1 and even components equal to 0.

2 MODEL ORDER REDUCTION BY MOMENT-MATCHING

We briefly recall in this section specific (and necessary) notions and definitions of moment-based theory. The reader is referred to key studies, such as (Astolfi 2010) or (Scarcioffi and Astolfi 2017b), where a detailed theoretical development of such concepts is provided.

Moments for linear systems

Consider a finite-dimensional, single-input, single-output, continuous-time system Σ described, for $t \geq 0$, by the state-space model

$$\Sigma: \begin{cases} \dot{x}(t) = Ax(t) + Bu(t) \\ y(t) = Cx(t) \end{cases} \quad (1)$$

where $x(t) \in \mathbb{R}^n$, $u(t) \in \mathbb{R}$, $y(t) \in \mathbb{R}$ are n -dimensional coordinates of a state-space manifold \mathcal{X} , and hence $A \in \mathbb{R}^{n \times n}$, $B \in \mathbb{R}^{n \times 1}$ and $C \in \mathbb{R}^{1 \times n}$. Consider the associated transfer function $W(s): \mathbb{C} \rightarrow \mathbb{C}$, computed in terms of the associated impulse response $w(t) = Ce^{At}B$, $w(t) \in L^2(\mathbb{R})$ as

$$\mathcal{L}\{w(t)\} \mapsto W(s) = C(s\mathbb{I}_n - A)^{-1}B \quad (2)$$

and assume that (1) is minimal (i.e. controllable and observable).

Definition 1. (Antoulas 2005) *The 0-moment of system (1) at $s_i \in \mathbb{C} \setminus \sigma(A)$ is the complex number*

$\eta_0(s_i) = C(s_i \mathbb{I}_n - A)^{-1} B$. The k -moment of system (1) at $s_i \in \mathbb{C}$ is the complex number

$$\eta_k(s_i) = \frac{(-1)^k}{k!} \left[\frac{d^k}{ds^k} (C(s \mathbb{I}_n - A)^{-1} B) \right]_{s=s_i}, \quad (3)$$

with $k \geq 1$ integer.

(Astolfi 2010) presents a new interpretation of moments in terms of the steady-state response of the output of the interconnection between a signal generator and system (1). This result is recalled, without a proof, in the following theorem (the reader is referred to (Astolfi 2010) for a comprehensive proof).

Theorem 1. (Astolfi 2010, Scarciotti and Astolfi 2017b, Scarciotti and Astolfi 2017a) Consider system (1) and the signal generator

$$\begin{aligned} \dot{\xi}(t) &= S \xi(t), \\ u(t) &= L \xi(t), \end{aligned} \quad (4)$$

with $\xi(t) \in \mathbb{R}^{\nu \times 1}$, $S \in \mathbb{R}^{\nu \times \nu}$, $L \in \mathbb{R}^{1 \times \nu}$ and $\xi(0) \in \mathbb{R}^{\nu \times 1}$. Assume that the triple $(L, S, \xi(0))$ is minimal, $\sigma(A) \subset \mathbb{C}^-$, $\sigma(S) \subset \mathbb{C}^0$ and the eigenvalues of S are simple. Let $\Pi \in \mathbb{R}^{n \times \nu}$ be the (unique) solution of the Sylvester equation

$$A\Pi + BL = \Pi S. \quad (5)$$

Then there exists a one-to-one relation between the moments $\eta_0(s_1)$, $\eta_0(s_2)$, ..., $\eta_0(s_\nu)$, with $s_i \in \sigma(S)$ for all $i=1, \dots, \nu$, and the steady-state response $C\Pi\xi$ of the output y of the interconnection of system (1) with the signal generator (4). In fact, the moments are uniquely determined by the matrix $C\Pi$.

Remark 1. The minimality of the triple $(L, S, \xi(0))$ implies the observability of (L, S) and the controllability of $(S, \xi(0))$.

Remark 2. From now on, the matrix $C\Pi \equiv \bar{Y}$ is referred as the moment-domain equivalent of $y(t)$.

Assumption 1. We write the matrix S in a real block-diagonal form as

$$S = 0 \oplus \left(\bigoplus_{p=1}^f \begin{bmatrix} 0 & \omega_p \\ -\omega_p & 0 \end{bmatrix} \right), \quad (6)$$

where $\omega_p > 0$, $\nu = 2f + 1$, $f \geq 0$ integer.

Before going further with the theoretical background on moment-matching, we recall the following proposition, which allows the computation of the matrix $\bar{Y} = C\Pi$ in terms of the impulse response of system Σ .

Proposition 1. (Faedo et al. 2018) Consider the interconnection between system (1) and the signal generator (4). Without loss of generality, select the initial conditions of (4) as $\xi(0) = [1 | \varepsilon_{\nu-1}] \in \mathbb{R}^{\nu \times 1}$ so that the minimality condition on the triple $(L, S, \xi(0))$ holds as long as the pair (L, S) is observable. Then, under Assumption 1, the moment-domain equivalent \bar{Y} can be alternatively computed from the impulse response of system Σ as

$$\bar{Y} = L \mathcal{R}_w, \quad (7)$$

where the matrix \mathcal{R}_w can be written in block-diagonal form as,

$$\mathcal{R}_w = W(0) \oplus \left(\bigoplus_{i=1}^f \begin{bmatrix} \Re\{W(j\omega_p)\} & \Im\{W(j\omega_p)\} \\ -\Im\{W(j\omega_p)\} & \Re\{W(j\omega_p)\} \end{bmatrix} \right) \quad (8)$$

with $W(s) = \mathcal{L}\{w(t)\}$.

Lastly, the following key result is recalled from (Astolfi 2010, Scarciotti and Astolfi 2017b).

Theorem 2. (Astolfi 2010, Scarciotti and Astolfi 2017b) The family of systems described by

$$\tilde{\Sigma}: \begin{cases} \dot{\Theta}(t) = (S - GL)\Theta(t) + Gu(t), \\ \theta(t) = \bar{Y}\Theta(t), \end{cases} \quad (9)$$

parametrised on $G \in \mathbb{R}^{\nu \times 1}$, such as $\sigma(S - GL) \cap \sigma(S) = \emptyset$, contains all the models of dimension ν interpolating the moments of system (1) at $\sigma(S)$.

Remark 3. The transfer function of the reduced order model (9) interpolates the transfer function of system (1) at the eigenvalues of S . Equivalently, the steady-state output of the reduced order model (9) matches exactly the steady-state output of the system resulting from the interconnection between system (1) and the signal generator (4). Note that if Assumption 1 holds, the interpolation points effectively represents a set of frequencies $\{\omega_p\}$ in the complex plane.

Remark 4. The matrix G can be selected to enforce specific properties of the original system on the reduced order model, such as a set of prescribed eigenvalues, as detailed in (Astolfi 2010, Scarciotti and Astolfi 2017b).

3 WEC EQUATIONS OF MOTION

We consider a 1-DoF (degree of freedom) WEC in this study for clarity, since the extension of the proposed method to multiple degrees of freedom can be done in an analogous procedure.

Time-domain formulation

The linearised equation of motion for a 1-DoF device can be expressed in the time-domain in terms of Newton's second law, obtaining the following linear formulation:

$$m\ddot{x}(t) = \mathcal{F}_r(t) + \mathcal{F}_h(t) + \mathcal{F}_e(t), \quad (10)$$

where m is the mass of the device, $x(t)$ the device displacement, $\mathcal{F}_e(t)$ the wave excitation force, $\mathcal{F}_r(t)$ the radiation force and $\mathcal{F}_h(t)$ the hydrostatic restoring force. The linearised hydrostatic force for a floating body can be written as $\mathcal{F}_h(t) = -s_h x(t)$, where $s_h > 0$ denotes the hydrostatic stiffness. The radiation force $\mathcal{F}_r(t)$ is modelled using linear potential theory and, using the well-known Cummins' equation (Cummins 1962), is

$$\mathcal{F}_r(t) = -\mu_\infty \ddot{x}(t) - \int_0^{+\infty} k(\tau) \dot{x}(t - \tau) d\tau, \quad (11)$$

where $\mu_\infty = \lim_{\omega \rightarrow +\infty} A(\omega)$. $\mu_\infty > 0$ is the added-mass at infinite frequency, $A(\omega)$ the radiation added mass and $k(t) \in L^2(\mathbb{R})$ the (causal) radiation impulse response, containing all the memory effect of the fluid response. Finally, the complete linearised equation of motion of the WEC is given by

$$(m + \mu_\infty) \ddot{x}(t) + k(t) * \dot{x}(t) + s_h x(t) = \mathcal{F}_e(t), \quad (12)$$

The equation of motion (12) is of a Volterra integro-differential form of the convolution class. The internal stability of such an equation (for the WEC case) is guaranteed for any physically meaningful values of the parameters and the convolution kernel $k(t)$ involved (Falnes 2002).

Frequency-domain formulation

Since the mapping in (12) has a well-defined steady-state response, it is useful to derive a frequency-domain analysis of such a system. Applying the Fourier transform to (12), and considering velocity as the measurable output, the following representation

$$V(j\omega) = \mathcal{F}_e(j\omega) H(j\omega), \quad (13)$$

where $H(j\omega)$ represents the force-to-velocity frequency response, holds. $H(j\omega)$ is a function of a specific set of characteristic frequency-dependent parameters, namely

$$H(j\omega) = \frac{1}{B(\omega) + j\omega[A(\omega) + m] + \frac{s_h}{j\omega}}, \quad (14)$$

where $B(\omega)$ is the radiation damping of the device (Falnes 2002). The hydrodynamic parameters $A(\omega)$ and $B(\omega)$ can be efficiently obtained using BEM solvers, such as WAMIT or NEMOH.

Mapping between time and frequency

In (Ogilvie 1964), a direct relationship between time-domain (12) and frequency-domain (13) models is derived, as a function of the parameters $B(\omega)$ and $A(\omega)$, and the radiation kernel $k(t)$, using the definition of the Fourier transform, namely

$$\begin{aligned} B(\omega) &= \int_0^{+\infty} k(t) \cos(\omega t) dt, \\ A(\omega) &= \mu_\infty - \frac{1}{\omega} \int_0^{+\infty} k(t) \sin(\omega t) dt. \end{aligned} \quad (15)$$

Then, the impulse response $k(t): \mathbb{R} \rightarrow \mathbb{R}$ can be written as a mapping involving the frequency-dependent parameters as

$$k(t) = \frac{2}{\pi} \int_0^{+\infty} B(\omega) \cos(\omega t) d\omega. \quad (16)$$

Equation (16) allows a frequency-domain analysis of $k(t)$: a direct application of the Fourier transform, yields

$$K(j\omega) = B(\omega) + j\omega[A(\omega) - \mu_\infty]. \quad (17)$$

The radiation kernel frequency response $K(j\omega)$ has a set of particular properties, which have been used in the literature to enforce a structure on the parametric model used to identify the frequency domain data (see, for example, (Taghipour et al. 2008) and (Pérez and Fossen 2008)), in an attempt to improve the quality of the obtained model. Such properties are recalled from (Pérez and Fossen 2008) in Table 1.

This study addresses the identification of a finite-order parametric model for the radiation impulse kernel that respects the full set of properties stated in Table 1 (The reader is referred to (Taghipour et al. 2008) for a comprehensive demonstration of each property).

Remark 5. Note that the family of models (9) is inherently strictly proper. The stability condition can be guaranteed by choosing G such that (9) is stable (see Remark 4).

4 PARAMETRIC IDENTIFICATION OF K WITH PRESERVATION OF PASSIVITY

To understand the importance of the passivity condition of the radiation subsystem, we write the Laplace counterpart of (14) i.e. $H(s)$ as a feedback interconnection between $\hat{H}(s)$ and the radiation subsystem $K(s)$, as depicted in Figure 1, where

$$\hat{H}(s) = \frac{s}{(A+m)s^2 + s_h}, \quad (18)$$

And A is the radiation added-mass evaluated at a particular frequency (when $s = j\omega$). One of the fundamental properties behind passivity is that the negative feedback interconnection between passive systems is also passive and, hence, closed-loop stable (Khalil 1996). The transfer function $\hat{H}(s)$ is passive (Kristiansen et al. 2005) and therefore, the interconnection between $\hat{H}(s)$ and $K(s)$ will be passive as long as the latter transfer function is also passive, guaranteeing the stability of $H(s)$.

Remark 6. Note that the non-passivity of $K(s)$ does not necessary imply that $H(s)$ is unstable. Nevertheless, passivity is a physical property of radiation forces and should be respected by a suitable parametric approximation.

Motivated by this, we present, in the following, a passivity-preserving moment-matching based algorithm, that computes a passive finite-order approximation for the radiation force convolution term in (12).

4.1 Moment equivalent of the radiation system

The radiation convolution term in (11) defines a linear time-invariant system completely characterised by the impulse response function $k(t)$, where the input considered is the velocity of the device $\dot{x}(t)$, i.e.

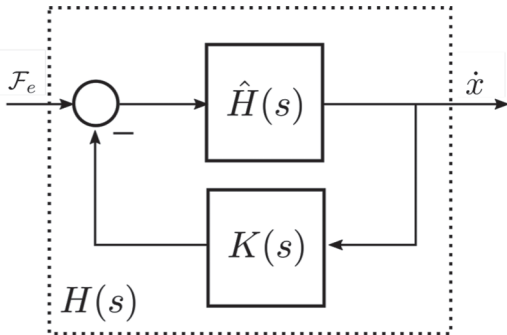


Figure 1. Feedback structure for $H(s)$.

$$y_k(t) = k(t) * \dot{x}(t). \quad (19)$$

A reduced order model, via moment-matching, can be obtained using the result on the moment-domain equivalent of a system, computed in terms of its impulse response, as in Proposition 1.

Assume that the velocity $\dot{x}(t)$ of the WEC can be written as a signal generator in implicit form, in a similar fashion to (4), expressed as a set of linear differential equations given by

$$\begin{aligned} \dot{\xi}_k(t) &= S\xi_k(t), \\ \dot{x}(t) &= L_k\xi_k(t), \end{aligned} \quad (20)$$

with $\xi_k(0) = [1 | \varepsilon_v]$ and L_k such as the pair (L_k, S) is observable. Then, recalling Proposition 1, the moment-domain equivalent of the output of (19) can be straightforwardly computed as $\bar{Y}_k = L_k \mathcal{R}_k$ where $\mathcal{R}_k \in \mathbb{R}^{v \times v}$ is a block-diagonal matrix defined by

$$\mathcal{R}_k = 0 \oplus \left(\bigoplus_{p=1}^f \begin{bmatrix} \Re\{K(j\omega_p)\} & \Im\{K(j\omega_p)\} \\ -\Re\{K(j\omega_p)\} & \Im\{K(j\omega_p)\} \end{bmatrix} \right), \quad (21)$$

Note that its entries depend on the added mass $A(\omega)$ and the radiation damping $B(\omega)$ of the device at each specific frequency induced by the eigenvalues of S , as

$$\begin{aligned} \Re\{K(j\omega_p)\} &= B(\omega_p), \\ \Im\{K(j\omega_p)\} &= \omega_p [A(\omega_p) - \mu_\infty]. \end{aligned} \quad (22)$$

A reduced order model of (19) can be obtained by applying Theorem 3. Specifically:

$$\tilde{\Sigma}_k : \begin{cases} \dot{\Theta}_k(t) = (S - G_k L_k) \Theta_k(t) + G_k \dot{x}(t), \\ \theta_k(t) = \bar{Y}_k \Theta_k(t), \end{cases} \quad (23)$$

is the family of reduced order models parametrised in G_k , interpolating the moments of system (19) at the eigenvalues of S , where $\bar{Y}_k = L_k \mathcal{R}_k$.

Remark 7. The reduced order model (23) has maximum dimension $v = 2f + 1$ (if $s_i = 0$ is chosen as an interpolation point), where f is the number of non-zero interpolation points (frequencies) selected. This is a consequence of the fact that, for each frequency ω_p , both $\pm j\omega_p$ (i.e. complex pole pairs) are chosen as eigenvalues of the real-valued matrix S .

4.2 Passivity preservation

We begin this subsection by recalling the basic concepts behind passivity.

Definition 2. (Passive system) (Khalil 1996) *A system Σ is said to be passive if $\Re \left\{ \int_{-\infty}^t u(\tau)y(\tau)d\tau \right\} \geq 0$ for all $t \in \mathbb{R}$ and all $u(t) \in L^2(\mathbb{R})$.*

An equivalent passivity condition can be given in terms of the transfer function $W(s)$ (2).

Theorem 3. (Khalil 1996) The system Σ is passive if and only if its transfer function $W(s)$ is positive real, i.e.

- $W(s)$ is Hurwitz and
- $W(j\omega) + W(-j\omega)^T \geq 0, \forall \omega \in \mathbb{R}^+$.

Assumption 2. *The radiation kernel transfer function $K(s) = \mathcal{L}\{k(t)\}$ is positive real.*

Under Assumption 1 and 2, we would like to find a passive finite-order model for $k(t)$, based on moment-matching. Consequently, we recall the following theorem, that guarantees the existence of a passive model within the family of models in Equation (9).

Theorem 4. (Ionescu and Astolfi 2010) *Consider the family of reduced order models (9). Let S in (4) be such that $\sigma(S)$ contains a subset of the zeros of $W(s)$. Then, the family of models (9) contains a passive model, i.e. there exists a G such that (9) is passive.*

Remark 8. *We know, as a hydrodynamic fact, that the transfer function of the radiation kernel $K(s)$ has at least one zero at the origin (see Table 1). This means that, if we select $s = 0$ as an eigenvalue of S in (23), there always exists a matrix G_k such that $\tilde{\Sigma}_k$ is passive.*

Theorem 4 (via Remark 8) secures the existence of a passive parametric model based on moment-matching. The problem now boils down to the selection of a suitable G_k . To achieve such an objective, we make use of the *scattering representation* of the system Σ .

Definition 3. (Scattering representation) (Desoer and Vidyasagar 1975) *The scattering representation of system $\Sigma(1)$ is defined as*

$$\Sigma^s : \begin{cases} \dot{x}(t) = (A - BC)x(t) + \sqrt{2}Bv(t) \\ z(t) = \sqrt{2}Cx(t) - v(t) \end{cases} \quad (24)$$

which is obtained by the following transformation:

$$\begin{aligned} v(t) &= (1/\sqrt{2})(u(t) + y(t)), \\ z(t) &= (1/\sqrt{2})(y(t) - u(t)). \end{aligned} \quad (25)$$

We consider this transformation of coordinates, since it provides a suitable condition for the

passivity of the original system Σ in terms of the L_2 -gain of its scattering representation Σ^s , as recalled in the following theorem.

Theorem 5. (Desoer and Vidyasagar 1975) *The scattering representation Σ^s of a passive linear system Σ has L_2 -gain ≤ 1 .*

Remark 9. *The L_2 -gain of system (1) is equal to its H_∞ -norm, i.e. $\|W(s)\|_\infty$.*

In the light of Theorems 4 and 5, we propose, in Section 4.3, an optimisation-based method to compute a passive parametric model for the radiation subsystem from (23).

4.3 Optimisation-based selection of G_k

Define the following transfer function of system (23) $\mathcal{L}\{\tilde{\Sigma}_k\}$ as

$$\tilde{K}(s) = \bar{Y} [sI_\nu - (S - G_k L_k)]^{-1} G_k. \quad (26)$$

In practice, the frequency-dependent device parameters are calculated using hydrodynamic codes at a finite number of frequencies on a set $\Omega_k = \{\omega_i\}$, $\omega_i \in [\omega_l, \omega_u]$, with a frequency step of $\Delta\omega_p$, where ω_l and ω_u represents the lower and upper bounds of the range, respectively. Define the complex-valued vectors $K\omega$, \tilde{K}_ω as,

$$K_\omega = \begin{bmatrix} K(j\omega_l) \\ \vdots \\ K(j\omega_i) \\ \vdots \\ K(j\omega_u) \end{bmatrix}, \quad \tilde{K}_\omega = \begin{bmatrix} \tilde{K}(j\omega_l) \\ \vdots \\ \tilde{K}(j\omega_i) \\ \vdots \\ \tilde{K}(j\omega_u) \end{bmatrix}. \quad (27)$$

Let $\tilde{\Sigma}_k^s$ be the scattering representation of system $\tilde{\Sigma}_k$ in (23). Then, we propose an optimisation-based procedure to select the matrix G_k by selecting a suitable set of eigenvalues $\Lambda_k \subset \mathbb{C}^-$ and preserving passivity at the same time, i.e.:

$$\min_{\Lambda_k \subset \mathbb{C}^-} \|K_\omega - \tilde{K}_\omega\|_2^2.$$

subject to

$$\begin{aligned} \|\mathcal{L}\{\tilde{\Sigma}_k^s\}(s)\|_\infty &\leq 1, \\ \|L_k \mathcal{R}_k G_k\|_2 &\geq \gamma, \quad \gamma \in \mathbb{R}^+. \end{aligned} \quad (28)$$

Remark 10. *Note that solving for Λ_k actually solves for G_k , since system (23) is controllable (Astolfi 2010) and hence there is a unique G_k such that $\sigma(S - G_k L) = \Lambda_k$.*

Remark 11. We assume that $s = 0$ is selected as an eigenvalue of the matrix S , so that the existence of a passive model is guaranteed by Theorem 4 (see Remark 6). The remainder of the interpolation points (frequencies) can be selected by the user in a sensible manner, as discussed in (Faedo et al. 2018).

Remark 12. The optimisation process consists of selecting a set of eigenvalues to minimise the ℓ_2 distance between the frequency response of the parametric model and the target frequency domain data, while ensuring that the obtained model is passive by constraining the L_2 -gain of its scattering representation.

Remark 13. The constraint $\|L_k \mathcal{R}_k G_k\|_2 \geq \gamma$ guarantees that the obtained model $\tilde{\Sigma}_k$ has relative degree 1 (see (Astolfi 2010)) as specified in Table 1.

Remark 14. BEM solvers can have numerical errors, resulting in hydrodynamic data that erroneously represents a non-passive system (e.g. radiation damping $B(\omega)$ with negative values) (Penalba et al. 2017). Our strategy attempts to deal with these singularities and is used to “fix” the target frequency-domain data so that the emerging parametric model is passive.

5 NUMERICAL EXAMPLE

We consider the hydrodynamic coefficients of the float of the OPT WEC device (see (Penalba et al. 2017) and Figure 2) to present a direct application of the proposed method. Our choice of device is merely justified by the geometrical complexity of such a WEC, which presents a multimodal frequency response, as can be appreciated in the subsequent Bode plots. The frequency range considered to compute the approximation (see Equation (28)) is set to $\omega_l = 0.3$ and $\omega_u = 3$.

We first compute a moment-matching based parametric model solving the unconstrained version of the optimisation procedure (28) (i.e. the basic method developed in (Faedo et al. 2018)), using as interpolation points the frequencies 0.3, 1 and 2.3. With this device, this selection of points,

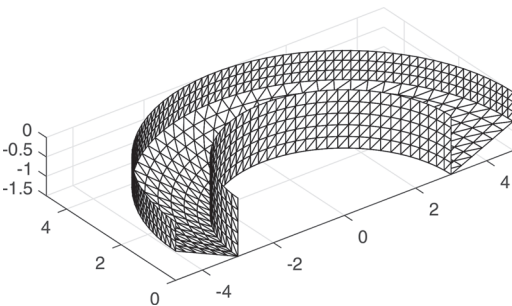


Figure 2. Low-order mesh of the OPT WEC float.

and the specific frequency range, the parametric approximation computed with the moment-matching method presented in (Faedo et al. 2018) is non-passive. Therefore, we proceed with the computation of a parametric approximation using the constrained formulation (28) developed in this study. Following Remark 4, we replace the interpolation point $\omega = 0.3$ by $\omega = 0$. The passivity condition can be checked using the frequency response of the scattering representation of both models, which is depicted in Figure 3. The frequency response of both approximations can be appreciated in Figure 4.

Figure 3 explicitly illustrates the passivity violation for the first model (solid-blue): the L_2 -gain of its scattering representation is greater than one and, hence, the model is non-passive. This is not the case with the parametric model computed with

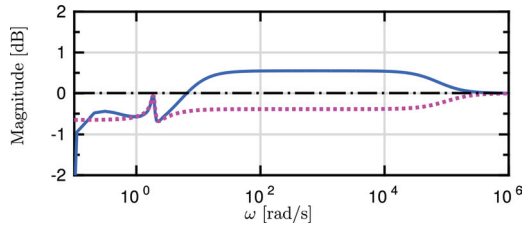


Figure 3. Bode diagram of the transfer function of the scattering representation of the non-passive (solid-blue) and passive (dotted-pink) parametric models.

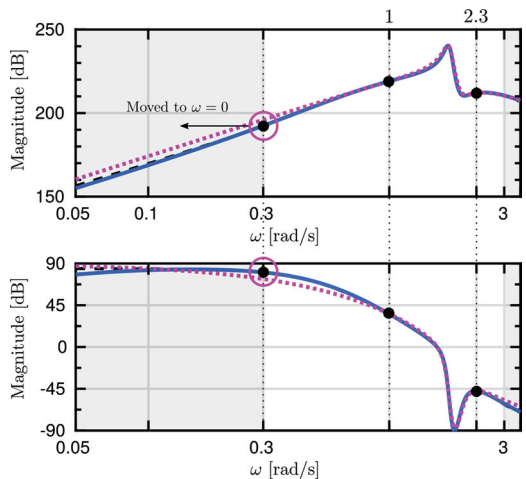


Figure 4. Bode diagram of the target frequency response (dashed-black), a non-passive parametric model achieving moment-matching at $\{0.3, 1, 2.3\}$ (solid-blue) and a passive parametric model achieving moment-matching at $\{0, 1, 2.3\}$ (dotted-pink). The interpolation points are marked with black dots.

the strategy proposed in this study (dotted-pink), which has a scattering representation with L_2 -gain less or equal than 1 and, hence, is passive.

Figure 4 depicts the Bode plot of the target frequency-domain data, and the frequency response of both the non-passive and passive models computed for this example. Note that the non-passive model has order 6 (twice the number of interpolation frequencies selected) while the passive model has order 5. This (partially) explains the difference of accuracy between both models within the frequency range selected for the application. This difference can be minimised by selecting more interpolation points, as can be noted in the next example of this section.

Remark 15. *It is possible to equate the order of both models by matching (additionally) at the first order moment at $s = 0$ i.e. $\eta_i(0)$ (see Definition 1). Nevertheless, we consider only 0-order moments in this study to simplify the analysis.*

We now repeat the procedure but selecting a higher number of interpolation points in the moment-matching process. The set of frequencies to compute the unconstrained version of (28) (Faedo et al. 2018) is selected as $\{0.3, 1, 1.6, 1.8, 2.3, 2.8\}$ which renders, for this case, a non-passive model. Motivated by this, we replace the interpolation point $\omega = 0.3$ by $\omega = 0$ as in the previous example to compute a model under the strategy presented in this study. The passivity violation for the first model can be appreciated in the Nyquist diagram of Figure 5: a passive model has always positive real-part and, hence, a Nyquist plot only defined on the right half-plane. It can be acknowledged from Figure 5 how this strategy enforces the passivity condition in the parametric approximation (dotted-pink).

Finally, Figure 6 depicts the Bode plot of the target frequency-domain response and the last two discussed approximations i.e. the non-

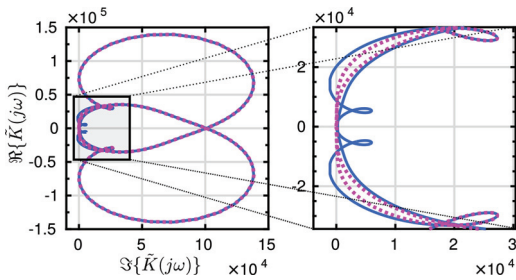


Figure 5. Nyquist diagram of a non-passive model achieving moment-matching at $\{0.3, 1, 1.6, 1.8, 2.3, 2.8\}$ (solid-blue) and passive model achieving moment-matching at $\{0, 1, 1.6, 1.8, 2.3, 2.8\}$ (dotted-pink).

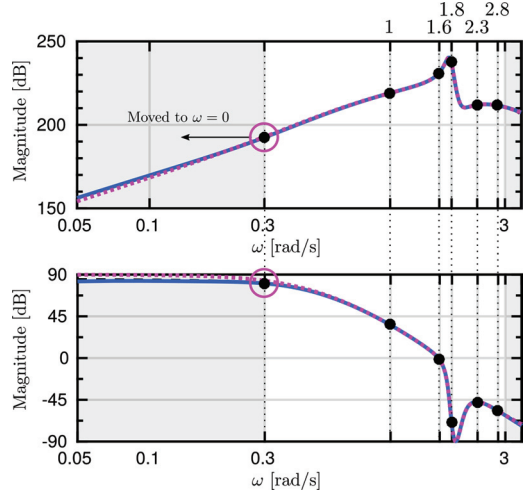


Figure 6. Bode diagram of the target frequency-response (dashed-black), a non-passive model achieving moment-matching at $\{0.3, 1, 1.6, 1.8, 2.3, 2.8\}$ (solid-blue) and a passive model achieving moment-matching at $\{0, 1, 1.6, 1.8, 2.3, 2.8\}$ (dotted-pink).

passive model achieving moment-matching at $\{0.3, 1, 1.6, 1.8, 2.3, 2.8\}$, and the passive model obtained with the optimised process (28) (replacing the interpolation frequency 0.3 by 0). It can be appreciated that the accuracy of the passive model increases considerably compared to the case presented in Figure 4 which, as discussed previously in this same section, is a consequence of the increase in the order of the approximating model.

6 CONCLUSIONS

A basic moment-matching based algorithm has been presented in (Faedo et al. 2018) that can be used to compute a parametric approximation for the radiation force convolution term of (12). Though usually the obtained approximations are inherently passive, the method developed in (Faedo et al. 2018) does not guarantee the passivity property, which can affect the internal stability of (12). This study introduces a modification of the basic algorithm which systematically ensures passivity within an optimisation process. We propose a method that secures the existence of a passive model by moment-matching and a suitable algorithm to effectively compute such an approximation, while retaining the desirable capability of selecting key frequencies in the interpolation process. The efficacy of the method is illustrated in terms of a numerical example, that approximates the radiation kernel of the float of the OPT device

(which has a multimodal frequency response) depicting an efficient method to systematically compute a passive parametric form.

ACKNOWLEDGMENTS

This material is based upon works supported by Science Foundation Ireland under Grant no. 13/IA/1886.

REFERENCES

- Antoulas, A.C. (2005). *Approximation of large-scale dynamical systems*. SIAM.
- Astolfi, A. (2010). Model reduction by moment matching for linear and nonlinear systems. *IEEE Transactions on Automatic Control* 55(10), 2321–2336.
- Babarit, A. & G. Delhommeau (2015). Theoretical and numerical aspects of the open source BEM solver NEMOH. In *11th European Wave and Tidal Energy Conference, Nantes*.
- Bacelli, G. & J.V. Ringwood (2015). Numerical optimal control of wave energy converters. *IEEE Transactions on Sustainable Energy* 6(2), 294–302.
- Cummins, W. (1962). The impulse response function and ship motions. Technical report, DTIC Document.
- Damaren, C.J. (2000). Time-domain floating body dynamics by rational approximation of the radiation impedance and diffraction mapping. *Ocean Engineering* 27(6), 687–705.
- Desoer, C.A. & M. Vidyasagar (1975). *Feedback systems: inputoutput properties*, Volume 55. Siam.
- Faedo, N., S. Olaya, & J.V. Ringwood (2017). Optimal control, mpc and mpc-like algorithms for wave energy systems: An overview. *IFAC Journal of Systems and Control* 1, 37–56.
- Faedo, N., Y. Peña-Sanchez, & J.V. Ringwood (2018). Finiteorder hydrodynamic model determination for wave energy applications using moment-matching. *Ocean Engineering* 163, 251–263.
- Faedo, N., G. Scarcioiti, A. Astolfi, & J.V. Ringwood (2018). Energy-maximising control of wave energy devices using a moment-domain representation. *Control Engineering Practice (under review)*.
- Falnes, J. (2002). *Ocean waves and oscillating systems: linear interactions including wave-energy extraction*. Cambridge university press.
- Ionescu, T.C. & A. Astolfi (2010). On moment matching with preservation of passivity and stability. In *Decision and Control (CDC), 2010 49th IEEE Conference on*, pp. 6189–6194.
- Khalil, H.K. (1996). *Nonlinear Systems*. Prentice-Hall, New Jersey.
- Kristiansen, E., Å. Hjulstad, & O. Egeland (2005). State-space representation of radiation forces in time-domain vessel models. *Ocean Engineering* 32(17), 2195–2216.
- Lee, C.-H. (1995). *WAMIT theory manual*. Massachusetts Institute of Technology, Department of Ocean Engineering.
- Ogilvie, T.F. (1964). Recent progress toward the understanding and prediction of ship motions. In *5th Symposium on naval hydrodynamics*, Volume 1, pp. 2–5. Bergen, Norway.
- Penalba, M., T. Kelly, & J.V. Ringwood (2017). Using NEMOH for modelling wave energy converters: A comparative study with WAMIT. In *Proceedings of the 12th European Wave and Tidal Energy Conference, Cork*. 12th European Wave and Tidal Energy Conference.
- Pérez, T. & T.I. Fossen (2008). Time-vs. frequency-domain identification of parametric radiation force models for marine structures at zero speed. *Modeling, Identification and Control* 29(1), 1–19.
- Roessling, A. & J.V. Ringwood (2015). Finite order approximations to radiation forces for wave energy applications. *Renewable Energies Offshore*, 359.
- Scarcioiti, G. & A. Astolfi (2017a). Data-driven model reduction by moment matching for linear and nonlinear systems. *Automatica* 79, 340–351.
- Scarcioiti, G. & A. Astolfi (2017b). Nonlinear model reduction by moment matching. *Foundations and Trends in Systems and Control* 4(3–4), 224–409.
- Taghipour, R., T. Perez, & T. Moan (2008). Hybrid frequency–time domain models for dynamic response analysis of marine structures. *Ocean Engineering* 35(7), 685–705.